

Alternative Indices for the Warm-Season NAO and Precipitation Variability in West Greenland

FRANK A. AEBLY, QI HU, AND SHERILYN C. FRITZ

Department of Geosciences, University of Nebraska–Lincoln, Lincoln, Nebraska

(Manuscript received 11 October 2006, in final form 1 June 2007)

ABSTRACT

Observed precipitation records from Kangerlussuaq, Greenland, and atmospheric variables from the NCEP–NCAR reanalysis were used in a statistical analysis to elucidate controls on the seasonal variation of precipitation and develop indices that may be potentially useful for analyzing precipitation variability in paleoclimate and future climate change investigations. Three distinct patterns of correlation between precipitation and the 500-hPa geopotential height were found to represent three dominant atmospheric patterns that strongly influence precipitation for different times of the year. All three patterns show a relation to the North Atlantic Oscillation signature found in the first empirical orthogonal function of the 500-hPa height field. Spatially dependent indices were developed based on the 500-hPa geopotential field. The correlation coefficients between precipitation at Kangerlussuaq and these indices range from -0.38 for winter to 0.64 for the warm season (May–September). The warm-season index herein is the first index reported in the literature that correlates significantly with precipitation during the warm season. Correlations of these indices with precipitation in Oslo, Norway, are high and are of opposite sign to west Greenland indices for the winter and summer months. This indicates that they are good representations of the atmospheric patterns associated with the North Atlantic Oscillation and the west Greenland–northern Europe “seesaw.” High correlations are also found with precipitation measured at Nuuk, Qaqortoq, and Upernavik, Greenland.

1. Introduction

Regional precipitation variability is the most difficult climate variable to predict, yet it is critical for understanding the hydrologic cycle and budget. In Greenland, knowing the controls on precipitation variability is also important for understanding past growth and decay of the ice sheet and for modeling the future of the ice sheet in response to global climate change. It is generally accepted that precipitation in Greenland depends largely on synoptic-scale processes and the configuration of tropospheric waves; specifically, the North Atlantic Oscillation (NAO) has a major influence on winter precipitation variability over much of Greenland (Appenzeller et al. 1998b; Bromwich et al. 1999; Chen et al. 1997). The NAO index represents the variation in strength and position of the Icelandic low and Azores

high, and the station-based index is calculated as the normalized difference in sea level pressure between Stykkisholmur, Iceland, and Lisbon, Portugal (Hurrell 1995). During weak or negative NAO modes, meridional flow in the North Atlantic is increased and mid-latitude cyclones tend to track north, while during positive modes flow is more zonal and cyclones tend to track east toward western Europe. Temporal fluctuations in these patterns are responsible for the winter “seesaw” between west Greenland and northwest Europe (Barlow et al. 1997; Dawson et al. 2003). About 45% of the variability in winter precipitation over Greenland can be attributed to the NAO when precipitation is calculated from vertical motion and averaged over large portions of the island (Bromwich et al. 1999). In contrast, correlations between the NAO index and summer precipitation are weak, and, as a result, summer precipitation has received little attention in the scientific literature. This is ironic because precipitation during the summer months of June–August (JJA) accounts for 43% of annual precipitation, and December–March (DJFM) precipitation accounts for less than

Corresponding author address: Dr. Frank A. Aebly, Department of Geosciences, University of Nebraska–Lincoln, Lincoln, NE 68588-0340.
E-mail: faebly1@bigred.unl.edu

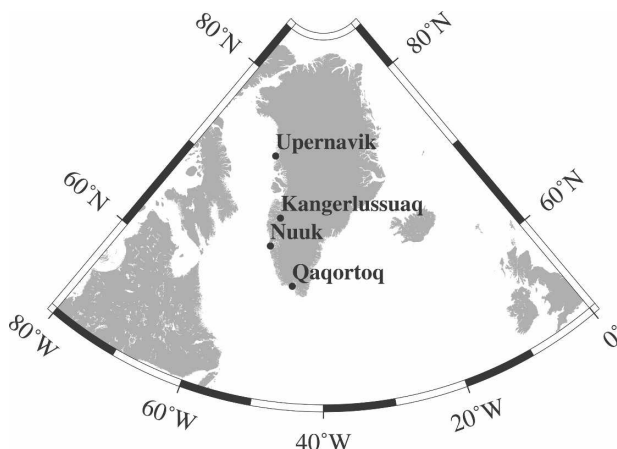


FIG. 1. Location map showing Kangerlussuaq and other stations listed in Table 4.

17% in parts of west Greenland; overall, the north, central, and west-central regions of Greenland receive their highest precipitation from May to October (Bromwich et al. 1999, their Fig. 3).

The NAO index has been correlated with paleoclimate proxies from ice sheets and tree rings that, in turn, have been used to extend the record of the NAO back to prehistoric times (Barlow et al. 1993; White et al. 1997; Appenzeller et al. 1998a). However, many recent high-resolution Holocene records of paleoclimate in west Greenland are derived from lake sediments, and most strongly reflect spring and summer environmental conditions (e.g., pollen, diatoms, and chironomids), particularly precipitation variability. Therefore, statistical indices that capture the warm-season precipitation variability in west Greenland would provide a valuable tool for both the paleoclimate and the hydrologic communities.

To better characterize the seasonality of the NAO, Portis et al. (2001) derived a “mobile” NAO index (NAOm) by using the points of maximum negative correlation between subtropical and subpolar sea level pressures. The index was termed mobile because, for each month of the year, the locations of maximum negative correlation migrated across the Atlantic. Although no attempt at correlating the NAOm with precipitation was made, the authors demonstrated that a spatially varying NAO index is more highly correlated with westerly winds and can provide better predictive capability in the North Atlantic region than the traditional NAO index.

This paper reports on a systematic statistical investigation of precipitation at Kangerlussuaq, west Greenland (Fig. 1), and of North Atlantic regional atmospheric variables. The focus of this study is the area

around Kangerlussuaq because it is the largest ice-free area of west Greenland and is the study site for several paleoclimate and limnology studies. Additionally, it has one of the longest precipitation records and is the location of the only international airport in west Greenland. Based on the premise that precipitation in west Greenland is largely a result of cyclonic activity (Chen et al. 1997), and that 500-hPa represents the “steering” level for cyclones, this study focused on atmospheric variability at this level. The purpose of this study is to develop statistical indices for the warm season that capture the variability in observed precipitation in west Greenland. Because of the error inherent in observed precipitation measurements, we first examine the pattern of correlation between winter precipitation and atmospheric variables for a NAO signature comparable to what has been reported using calculated precipitation (Bromwich et al. 1999). In section 3, we analyze the patterns of the correlation coefficient isopleths (hereafter referred to as isopleth patterns) for other months to determine the spatial variability of the centers of influence and derive normalized difference indices similar to those of the NAOm of Portis et al. (2001), but for seasonally averaged values. The isopleth patterns are compared to the empirical orthogonal functions (EOFs) of the 500-hPa height field in section 4. In section 5, we compare the correlations between precipitation, the developed indices, the principal components of the 500-hPa height field, and the Hurrell (1995) NAO indices at Kangerlussuaq, as well as other stations in west Greenland and western Europe. Conclusions are given in section 6.

2. Data and methods

Monthly values from 1950 to 2003 of the geopotential height (h), vertical motion (ω), and meridional (v) and zonal (u) wind at 500 hPa were obtained from the National Centers for Environmental Prediction–National Center for Atmospheric Research (NCEP–NCAR) 40-Year Reanalysis (Kalnay et al. 1996) dataset [National Oceanic and Atmospheric Administration–Cooperative Institute for Research in Environmental Sciences (NOAA–CIRES) Climate Diagnostics Center; information online at <http://www.cdc.noaa.gov/>]. The advantage of using reanalysis data is that even though it is considered “observed,” it is an assimilation of actual observations and modeled data. The model used for the reanalysis project accounts for interactions between the atmosphere, land, and water; clouds; boundary layer dynamics; and surface hydrology (Kalnay et al. 1996). The vertical component of relative vorticity (ζ) at 500 hPa was calculated using the “hcurl” function of

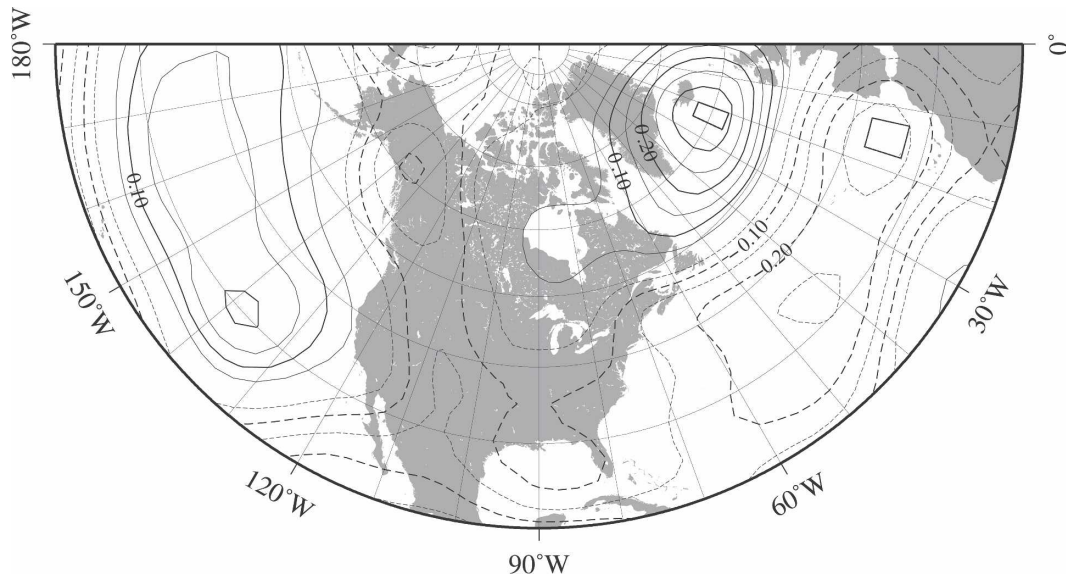


FIG. 2. The correlation isopleth map for JFM. Boxes outline the nine grid points used to calculate the 500-hPa index (see Table 2); the contour interval is 0.05, and the zero line is suppressed.

the Grid Analysis and Display System (GrADS; available online at <http://www.iges.org/grads/>).

Instrumental records of monthly precipitation at Kangerlussuaq, west Greenland, were obtained from the Danish Meteorological Institute (DMI; Cappelen et al. 2001) for 1976–99. In addition, instrumental data from 1950–70 and 1994–2003 were obtained from the Global Historical Climatology Network, version 2 (GHCN2) database, which is available from the U.S. National Climate Data Center (online at <http://www.ncdc.noaa.gov>). The average of the two records was used for the period of overlap (1994–99). No instrumental records for 1971–75 could be located, so this time period was excluded in our analyses.

Correlation coefficients between precipitation at Kangerlussuaq and h , ζ , v , u , and ω were calculated on $2.5^\circ \times 2.5^\circ$ grids over the North Atlantic region for each month, and isopleth maps were constructed. The periods of January–March (JFM), May–September (MJJAS), and October–November (OND) were determined based on the similarity of the spatial structure of the isopleths for each month. Seasonal averages of the atmospheric variables and total accumulated precipitation for each season were then used to create a second set of correlation coefficient isopleth maps. Normalized difference indices were then calculated for each variable using the average value of nine grid points centered on the highest positive and negative correlation coefficient. Averages were weighted by the cosine of latitude to account for the convergence of the meridians.

The indices calculated as described above were used in forward stepwise linear regression to determine which variable(s) (among h , ω , u , v , and ζ) contribute the most to observed precipitation variability, and to avoid multicollinearity between the variables. Of the variables evaluated, h was consistently the best predictor of precipitation, with little or no increase in explained variance for the other variables; therefore, all further discussion is concerned only with the 500-hPa height field.

3. Correlation isopleth maps

a. JFM

During the months of January–March, the isopleths exhibit a dipole pattern, with strong positive values near Iceland and strong negative values off the coast of Spain (Fig. 2). Consistently, this is also observed in the correlations of ζ with precipitation, but with strong negative values near Iceland and positive values over the North Atlantic. This winter pattern is a clear reflection of the NAO and is in agreement with studies showing that wet and warm winters in west Greenland are associated with a weak or reversed NAO pattern (Barlow et al. 1997; Dawson et al. 2003). A weak or reversed NAO results in increased meridional winds and the advection of warm, moist air toward Greenland. During a reversed NAO, a blocking ridge over the North Atlantic further enhances this advection, and midlatitude cyclones track north toward the Davis Strait. The relatively low correlation coefficient for the negative center

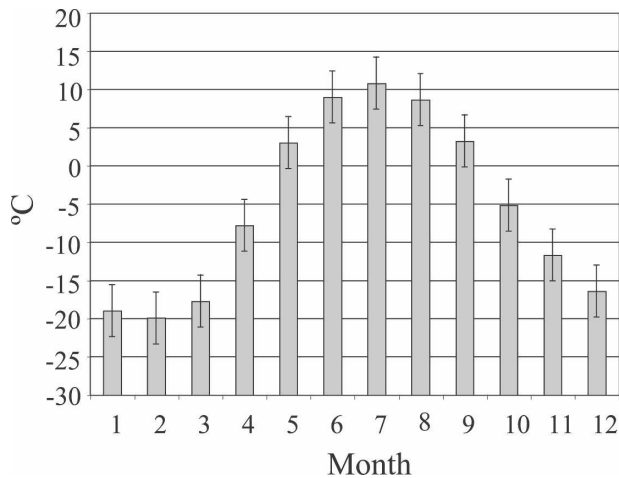


FIG. 3. The monthly mean temperature distribution for Kangerlussuaq. Vertical bars represent one standard error.

suggests that the steering associated with the high pressure ridge is a dominant factor in precipitation variability. This strong NAO signature lends confidence in using the observed precipitation values for evaluating the climate of the Kangerlussuaq region.

b. MJJAS

During the spring and summer months the centers of influence move north and west across the North Atlantic. Although May and September are not part of the celestial summer, this group includes the wettest periods on record, and the mean temperatures for May and September indicate that most of the precipitation in

those months is liquid (Fig. 3). In this sense, these months can be considered warm-season precipitation months. Furthermore, in examining the monthly correlation grids, we found that conditions at the 500-hPa level that exert an influence on precipitation in the summer are largely in place by May and remain in place through September. The MJJAS isopleth pattern is dominated by a dipole over Hudson Bay and northwest Greenland (Fig. 4), indicating that precipitation is strongly influenced by upstream atmospheric processes over northeast Canada and the Davis Strait. Novak et al. (2002) describe local maxima in cutoff cyclones from May to August 1953–99, located in the vicinity of eastern Baffin Island, Baffin Bay, and the Davis Strait; Serreze et al. (2001) show that cyclones generated over northern Alaska and Canada during the summer months track toward Greenland. The isopleth pattern for MJJAS may represent a combination of cyclone genesis, steering, and increased intensity in the Hudson Bay–Baffin Island area associated with the summer arctic frontal zone. This notion is supported by storm data obtained from National Aeronautic and Space Administration's (NASA's) Goddard Institute of Space Science (GISS). The number of cyclones and the average storm intensity (defined by central sea level pressure) reported in the database within the Hudson Bay–Baffin Island area (north of 60°N, between 100° and 60°W) were extracted and compared for the wettest and driest summer months from 1961 to 1998 (Table 1). With the exception of August 1991, the number of storms reported in the area is greater for the wet years than the dry years. Perhaps more importantly, the mean

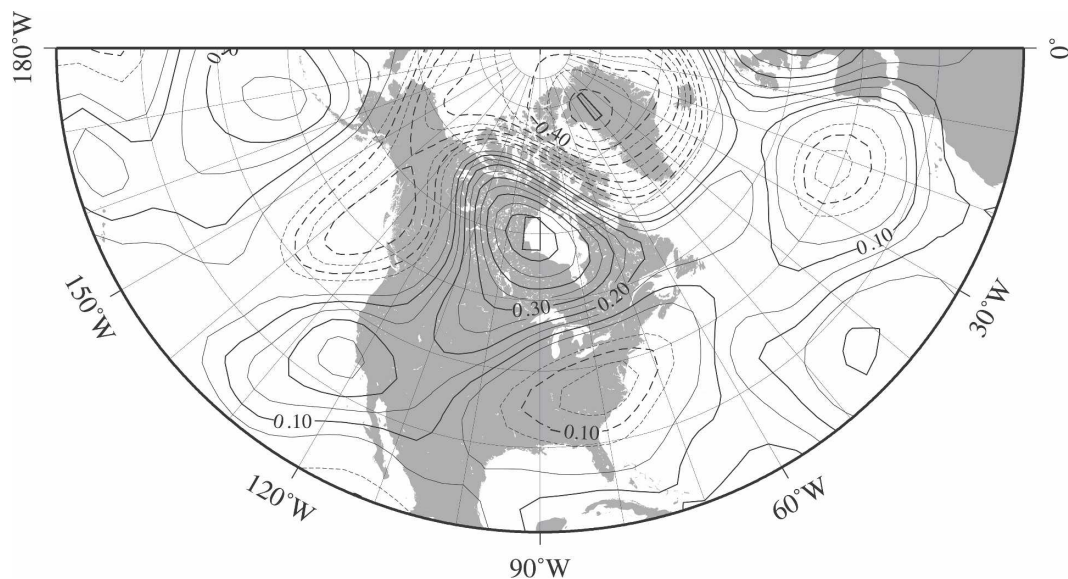


FIG. 4. As in Fig. 2, but for MJJAS.

TABLE 1. Precipitation and storm statistics for average conditions and months with the least (driest) and most (wettest) precipitation on record. Mean and standard deviations of average conditions are the long-term statistics for 1961–98; mean storm intensity for the extreme months is the mean storm intensity for that month and year. Storm data are from the GISS extratropical cyclone database, and are for the Hudson Bay–Baffin Island area (north of 60°, between 100° and 60°W). Storm intensity is defined by the central sea level pressure.

	Average conditions									
	May	June	July	August	September					
Mean precipitation (mm)	9.5	14.7	24.7	27.4	20.2					
Mean no. of storms	10.94	10.82	11.74	17.68	15.68					
Std dev (σ)	4.4	6.12	6.44	7.32	7.11					
Mean storm intensity (mb)	998.19	995.68	995.16	993.89	991.79					
Std dev (σ)	4.07	4.16	3.87	2.79	4.16					
	Conditions during extreme months									
	May		June		July		August		September	
	Dry	Wet	Dry	Wet	Dry	Wet	Dry	Wet	Dry	Wet
Year	1980	1961	1992	1994	1965	1997	1977	1991	1995	1967
Precipitation (mm)	0.0	32.5	1.6	39.6	8.6	98.5	0.0	80.4	3.0	51.3
No. of storms	16	19	11	17	5	9	16	14	17	27
Mean storm intensity (mb)	997.92	999.37	995.91	994.76	1001.69	989.00	997.67	988.66	992.82	984.92

storm intensity shows a marked increase for the wet months of July, August, and September, represented by a reduction in central pressure from 1.65σ to 1.88σ (σ is the standard deviation), and the difference in mean intensity between dry and wet years ranges from 1.9σ to 3.28σ . The GISS data demonstrate that wet summer months are associated with increased intensity or frequency of storms in the area. This observation is consistent with Cappelen et al. (2001), who observed that summer storms frequently come directly onto Greenland's west coast from the Baffin Island area. This storm track is considered secondary by Chen et al. (1997). With over 60% of the annual precipitation oc-

curing between May and September, the storm-track pattern clearly plays a more important role in annual precipitation for west Greenland than previously thought.

c. OND

Precipitation from October to December accounts for an additional 32.4% of annual precipitation, and the correlation pattern in OND is similar to that in JFM, except the dipoles have shifted west with the positive center located off the coast of Newfoundland and the negative center over the mid-Atlantic (Fig. 5). As for the JFM pattern, the correlation coefficient for the

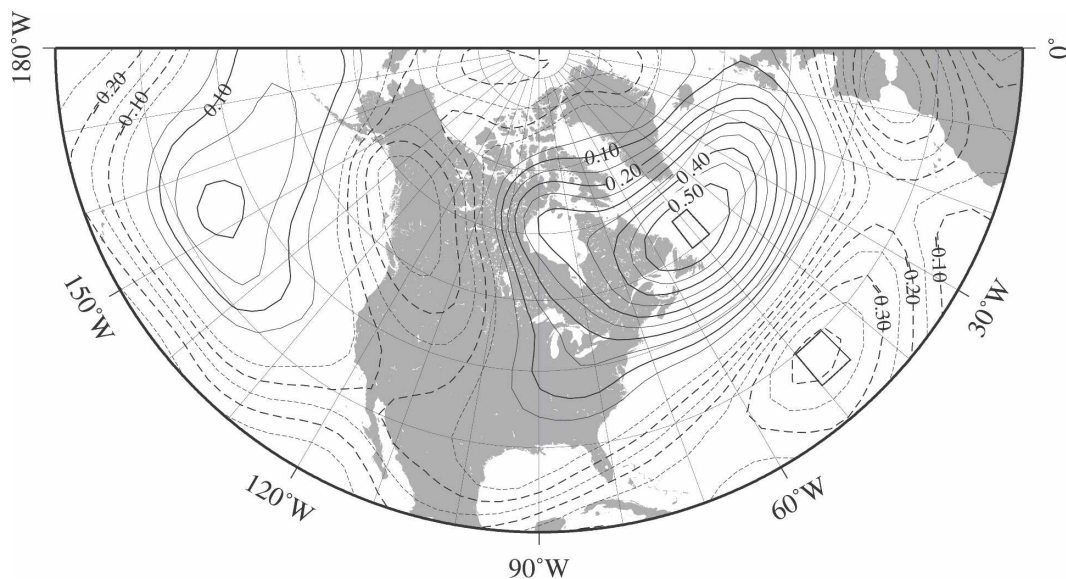


FIG. 5. As in Fig. 2, but for OND.

negative center is comparatively low, suggesting that a blocking ridge over the Goose Bay–Labrador Sea area and the associated veering of weather systems up the Davis Strait is a dominant factor in precipitation at Kangerlussuaq. This pattern is similar to that seen during negative winter NAO, but appears to be better developed along the western border of the North Atlantic Ocean. Thus, it would not be represented in the NAO index computed on the eastern side.

4. Relation to principal modes of the 500-hPa height field

EOFs were calculated over the entire Northern Hemisphere (NH) and for the Western Hemisphere, north of 20° (northwest quadrant). The relations between the isopleth patterns and the northwest quadrant EOF-1 loading patterns described below were largely similar to the relation with the EOF-2, when the EOFs were calculated over the entire NH. This is due to the dependence of EOF calculations on the spatial domain (Wilks 1995). The smaller northwest quadrant domain is used here because it better represents regional variability and smaller-scale shifts in the larger-scale atmospheric patterns, which are often responsible for surface climate (Yarnal and Diaz 1986). The isopleth maps and the EOF-1 loading pattern for each of the three seasons are shown in Fig. 6. In comparing the two patterns, it should be remembered that although the signs of the eigenvectors are arbitrary, those of the correlation coefficients are not.

EOF-1 for JFM clearly shows the NAO signature with a positive center over the southern tip of Greenland and a zonally extensive negative center over the North Atlantic. The isopleth pattern reflects the NAO signature seen in EOF-1. Although the maximum positive correlation occurs over Iceland and the maximum negative correlation is off the coast of Spain, the negative correlation coefficients are similar across the North Atlantic within the same region as the EOF-1.

The loading pattern of the MJJAS EOF-1 shows a large negative center over the North Pacific Ocean and a positive center over southern Greenland. However, the isopleth pattern corresponds to the weaker negative center just south of Hudson Bay, indicating that precipitation variability is responding to smaller perturbations of the larger atmospheric flow in the region. The large positive center and smaller and zonally extensive negative center is likely a manifestation of the weakened warm-season NAO, which tends to move north and west as insolation increases (Barnston and Livezey 1987).

By fall, the loading pattern of EOF-1 begins to resemble the Pacific–North America (PNA) pattern with a large positive center over the North Pacific Ocean and a large negative center over the western North America. The PNA pattern appears to dominate the variability of the 500-hPa surface during these months, but precipitation continues to respond to the NAO. The isopleth pattern resembles a western expression of the NAO as discussed above, and corresponds to the structure of the weaker centers of the OND EOF-1 over the North Atlantic Ocean.

5. Seasonal indices and their relation to precipitation in west Greenland

Using the locations of maximum correlation (see Table 2 and Figs. 2, 4, and 5), standardized difference indices of the 500-hPa height were calculated and analyzed for their correlations with seasonal and annual precipitation. The results are summarized in Table 3, along with those for the traditional station-based NAO indices provided by the Climate Analysis Section at NCAR (Hurrell 1995), and the first principal component of the 500-hPa field (PC-1). To account for autocorrelation, the correlation coefficients in Table 3 were tested for significance using effective degrees of freedom calculated using the method of Chen (1981), as presented in Livezey and Chen (1983). The effective degrees of freedom (n) are determined by

$$n = \frac{N\Delta t}{\tau}, \quad (1)$$

where N is the number of years in the series and τ is calculated as

$$\tau = [1 + 2 \sum_{i=1}^N C_{\text{panom}}(i\Delta t)C_{\text{pred}}(i\Delta t)]\Delta t. \quad (2)$$

Here, C_{panom} and C_{pred} are the autocorrelations of the precipitation anomaly and predictor variables, respectively, at lags $i\Delta t$ and $\Delta t = 1$. For any series with missing values, n was calculated for the longest continuous portion of the series, and then the effective degrees of freedom for the entire series were estimated using the proportion n/N . The significance levels reported in Tables 3 and 4 were determined using a two-tailed t test with the effective degrees of freedom.

The 500-hPa indices outperform all other predictors in that they are significant and have higher correlation coefficients than the other predictors for all seasons. Although Bromwich et al. (1999) obtained a higher correlation coefficient (-0.65) for JFM using the NAO index, they used calculated precipitation averaged over

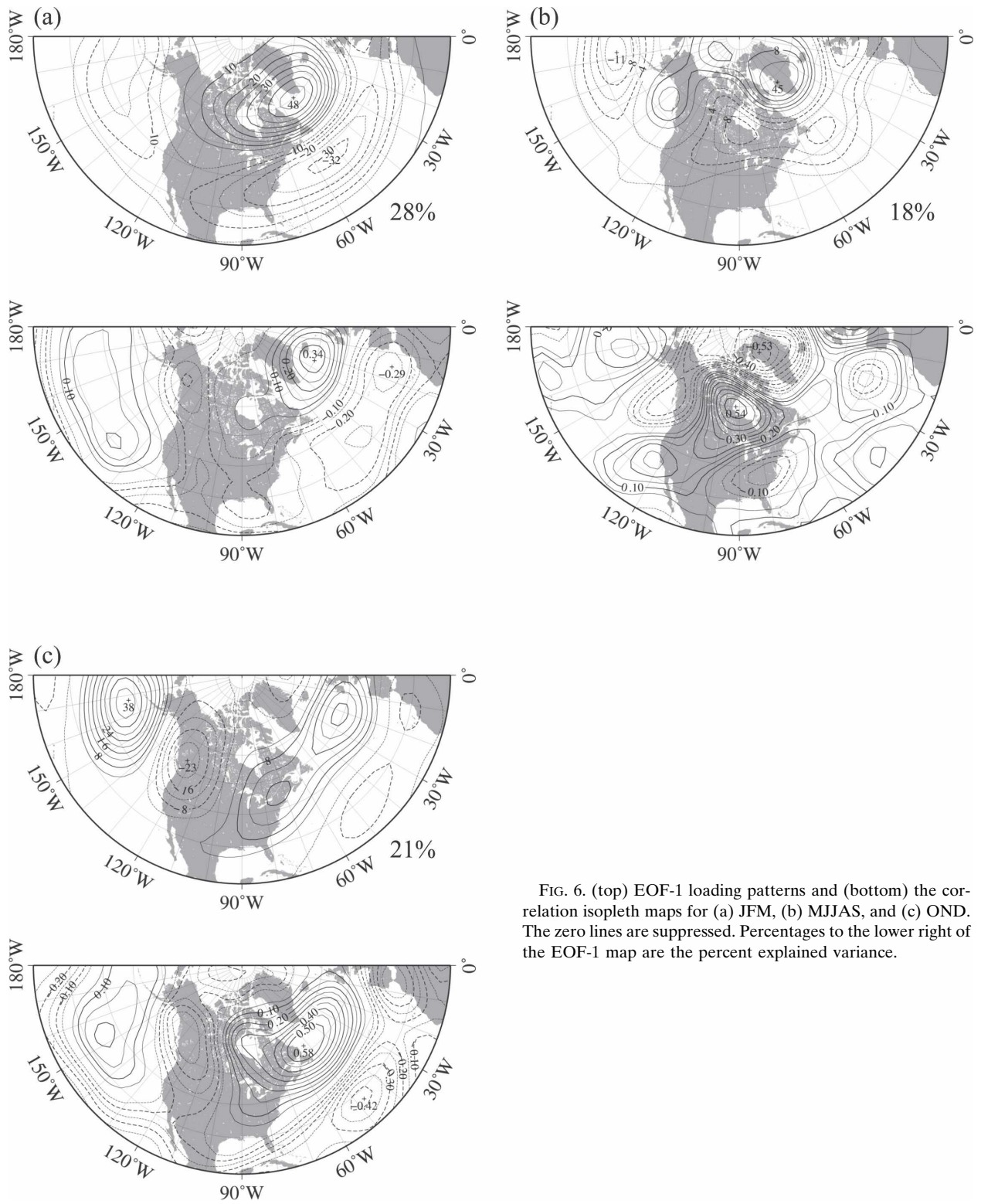


FIG. 6. (top) EOF-1 loading patterns and (bottom) the correlation isopleth maps for (a) JFM, (b) MJJAS, and (c) OND. The zero lines are suppressed. Percentages to the lower right of the EOF-1 map are the percent explained variance.

TABLE 2. Bounding boxes of the areas used for averaging of the 500-hPa h and calculation of the 500-hPa indices.

	JFM	MJJAS	OND
Area 1	32.5°N, 17.5°W; 37.5°N, 17.5°W; 37.5°N, 12.5°W; 32.5°N, 12.5°W	57.5°N, 95°W; 62.5°N, 95°W; 62.5°N, 90°W; 57.5°N, 90°W	25°N, 50°W; 30°N, 50°W; 30°N, 45°W; 25°N, 45°W
Area 2	57.5°N, 25°W; 62.5°N, 25°W; 62.5°N, 20°W; 57.5°N, 20°W	75°N, 52.5°W; 80°N, 52.5°W; 80°N, 47.5°W; 75°N, 47.5°W	50°N, 52.5°W; 55°N, 52.5°W; 55°N, 47.5°W; 50°N, 47.5°W

all of central west Greenland. The correlation coefficient for the NAO index is slightly lower than that for the 500-hPa index, and the p value is higher (0.086). The proposed index also correlates higher than PC-1 for MJJAS, explaining over one-third (0.64²) of the variation in summer precipitation at Kangerlussuaq. The 500-hPa indices show strong correlation with autumn and winter precipitation, whereas correlations with PC-1 are insignificant. Because precipitation at Kangerlussuaq appears to be responding to smaller-scale variability than the principal mode of the 500-hPa height field (see section 4), the correlations with the second and third principal components (PC-2 and PC-3, respectively) were also examined (not shown). PC-3 for both JFM and OND had higher correlation coefficients than PC-1 (−0.312 and 0.307, respectively), but significance levels remained lower than the 500-hPa indices.

To test these indices against other locations in Greenland, precipitation records from three other stations along the west coast and southern tip of Greenland (Fig. 1) were analyzed. Correlation coefficients between precipitation at the stations in Fig. 1 and the derived indices are shown in Table 4. Precipitation records from Oslo, Norway, were also examined be-

cause of the well-known winter seesaw between west Greenland and northern Europe. Reported p values were calculated using effective degrees of freedom as described above.

Nuuk, Greenland, located approximately 320 km southwest of Kangerlussuaq, experiences a more even monthly distribution of precipitation and a mean annual precipitation of 752 mm (Cappelen et al. 2001). Precipitation at Nuuk is highly correlated with the MJJAS and OND 500-hPa indices, with these seasons accounting for 50% and 25% of the annual precipitation, respectively. PC-1 is the only other predictor with significant correlation that is higher than the 500-hPa index for MJJAS, but does not correlate significantly with the other seasons. At the southern tip of Greenland, Qaqortoq receives on average 858 mm of precipitation annually. Southern Greenland is the wettest area on the island, and the MJJAS and OND precipitation at Qaqortoq are all highly correlated with the proposed 500-hPa indices, although significance for MJJAS is moderate. As in Nuuk, PC-1 for MJJAS exhibits higher correlation with MJJAS precipitation, but correlations with the other months are low. Upernavik receives a mean annual precipitation comparable to Kangerlussuaq (251 mm), and like Kangerlussuaq, receives the majority of this during the summer and fall, with very little winter precipitation. This location also has the shortest record among the stations investigated. The NAO index appears to be a better predictor of precipitation at Upernavik for JFM, with a highly significant correlation of −0.541, but does not show any significance for the wetter periods of the year. The 500-hPa indices for JFM and MJJAS correlate well with precipitation, but the coefficients are only moderately significant (0.05 < p < 0.10). The correlation coefficient for the JFM PC-1 is high, but because of the significant autocorrelation in the PC-1 and the short record, the coefficient is not significant.

As expected, the correlation between the JFM 500-hPa index and precipitation at Oslo is the reverse of that in west Greenland. Surprisingly, the MJJAS index also is correlated strongly with Oslo precipitation, and the correlation is opposite in sign to those of west Greenland. A direct relationship between precipitation

TABLE 3. Correlation coefficients between standardized precipitation anomalies, NAO indices, PC-1, and the 500-hPa indices for the three seasons discussed. (Bold coefficients: $p < 0.05$; *: $p < 0.10$; p values determined using effective degrees of freedom. See text for details.)

Predictor	Standardized precipitation anomalies at Kangerlussuaq		
	JFM	MJJAS	OND
500-hPa indices			
JFM	—	—	—
MJJAS	−0.38	—	—
OND	—	0.64	—
Hurrell (1995) NAO indices			
JFM	−0.31*	—	—
MJJAS	—	0.11	—
OND	—	—	0.04
PC-1			
JFM	0.144	—	—
MJJAS	—	−0.49	—
OND	—	—	0.294

TABLE 4. Correlation coefficients between standardized precipitation anomalies and the 500-hPa indices, NAO indices, and PC-1 for Nuuk (1958–98), Qaqortoq (1961–99), Upernavik (1958–80), Greenland, and Oslo, Norway (1950–96), are shown. (Bold coefficients: $p < 0.05$; *: $p < 0.10$; p values determined using effective degrees of freedom. See text for details.)

Predictors	Standardized precipitation anomalies											
	Nuuk			Qaqortoq			Upernavik			Oslo		
	JFM	MJJAS	OND	JFM	MJJAS	OND	JFM	MJJAS	OND	JFM	MJJAS	OND
500-hPa indices	—	—	—	—	—	—	—	—	—	—	—	—
JFM	-0.298	—	—	-0.189	—	—	-0.474*	—	—	0.540	—	—
MJJAS	—	0.433	—	—	0.402*	—	—	0.483*	—	—	-0.417	—
OND	—	—	-0.436	—	—	-0.489	—	—	-0.261	—	—	-0.076
Hurrell (1995)	—	—	—	—	—	—	—	—	—	—	—	—
NAO indices	—	—	—	—	—	—	—	—	—	—	—	—
JFM	-0.037	—	—	0.116	—	—	-0.541	—	—	0.343*	—	—
MJJAS	—	0.332	—	—	0.245	—	—	-0.150	—	—	0.054	—
OND	—	—	-0.097	—	—	-0.043	—	—	-0.085	—	—	0.282
PC-1	—	—	—	—	—	—	—	—	—	—	—	—
JFM	0.119	—	—	-0.046	—	—	0.424	—	—	-0.211	—	—
MJJAS	—	-0.521	—	—	-0.476	—	—	-0.341	—	—	0.379	—
OND	—	—	0.20	—	—	0.296	—	—	-0.042	—	—	-0.078

at Oslo and the configuration of the 500-hPa height field west of Greenland is not likely, given the large topographic barrier of the Greenland ice sheet. However, an indirect relationship associated with lower-latitude cyclones cannot be ruled out. A summer seesaw has not been described previously in the scientific literature, but these results suggest that this oscillation may warrant further investigation.

6. Conclusions

Statistical analyses were performed on a long record of precipitation in Kangerlussuaq and the atmospheric variables contributing to the variance in precipitation. The dominant predictor of those investigated was found to be the 500-hPa height field. Although this research did not consider the effects of sea surface temperature and ice cover on the variability of precipitation, the purpose of this research was to develop a univariate index that can be used for future investigations of warm-season precipitation variability, either with statistical downscaling of climate models or with associated relationships with warm-season-dependent climate proxy data. In addition to being the first such index to be developed, the proposed 500-hPa indices are also highly correlated with winter and fall precipitation at Kangerlussuaq.

Three distinct patterns are recognized in the correlations between precipitation and the 500-hPa geopotential height field. These patterns represent smaller perturbations in the larger-scale atmospheric circulation represented by the first EOF for each season, but also appear to be related to the NAO as it migrates and

strengthens/weakens through the year in response to solar heating and the contraction of the polar vortex (Barnston and Livezey 1987). During MJJAS, data from the GISS atlas of extratropical storm tracks suggest that the observed correlation is a result of increased cyclone frequency or intensity in the vicinity of Baffin Island, in agreement with previous studies. Because this season receives over 60% of the annual precipitation in Kangerlussuaq, an in-depth study of cyclogenesis and the effects of sea surface temperatures and ice cover in this region is warranted. Fall precipitation appears to be primarily controlled by a blocking ridge over the western North Atlantic, veering storms toward west Greenland much the same as the winter NAO. The station-based NAO index, with centers over the eastern North Atlantic, does not capture this variability.

The locations for calculating the proposed indices are allowed to migrate seasonally with the variation in solar heating and thus have greater skill at predicting precipitation in west Greenland than either the station-based NAO indices or the principal components of the 500-hPa height field. In addition, the indices also show a west Greenland–northern Europe seesaw, which suggests that this phenomenon occurs during the warm season.

Acknowledgments. We thank the editor and two anonymous reviewers for their helpful comments that have led to improvements of this manuscript. Thanks also go to John Anderson for providing the Kangerlussuaq data, and to David B. Radell for helpful discussions and assistance with the GrADS software. This

research was supported by NSF Grant ATM-0081226 to Sherilyn C. Fritz.

REFERENCES

- Appenzeller, C., T. F. Stocker, and M. Anklin, 1998a: North Atlantic Oscillation dynamics recorded in Greenland ice cores. *Science*, **282**, 446–449.
- , J. Schwander, S. Sommer, and T. F. Stocker, 1998b: The North Atlantic Oscillation and its imprint on precipitation and ice accumulation in Greenland. *Geophys. Res. Lett.*, **25**, 1939–1942.
- Barlow, L. K., P. M. Groote, J. W. C. White, R. G. Barry, and J. C. Rogers, 1993: The North Atlantic Oscillation signature in deuterium and deuterium excess signals in the Greenland Ice Sheet Project 2 ice core. *Geophys. Res. Lett.*, **20**, 2901–2904.
- , J. C. Rogers, M. C. Serreze, and R. G. Barry, 1997: Aspects of climate variability in the North Atlantic sector: Discussion and relation to the Greenland Ice Sheet Project 2 high-resolution isotopic signature. *J. Geophys. Res.*, **102**, 26 333–26 344.
- Barnston, A. G., and R. E. Livezey, 1987: Classification, seasonality and persistence of low-frequency atmospheric circulation patterns. *Mon. Wea. Rev.*, **115**, 1083–1126.
- Bromwich, D. H., Q. Chen, Y. Li, and R. I. Cullather, 1999: Precipitation over Greenland and its relation to the North Atlantic Oscillation. *J. Geophys. Res.*, **104**, 22 103–22 115.
- Cappelen, J., B. V. Jørgensen, E. V. Laursen, L. S. Stannius, and R. S. Thomsen, 2001: The observed climate of Greenland, 1958–99—With climatological standard normals, 1961–90. Danish Meteorological Institute Tech. Rep. 00-18, 152 pp.
- Chen, Q., D. H. Bromwich, and L. Bai, 1997: Precipitation over Greenland retrieved by a dynamic method and its relation to cyclonic activity. *J. Climate*, **10**, 839–870.
- Chen, W. Y., 1981: Fluctuations in Northern Hemisphere 700 mb height field associated with the Southern Oscillation. *Mon. Wea. Rev.*, **110**, 808–823.
- Dawson, A. G., and Coauthors, 2003: Late-Holocene North Atlantic climate ‘seesaws’, storminess changes and the Greenland ice sheet (GISP2) palaeoclimates. *Holocene*, **13**, 381–392.
- Hurrell, J. W., 1995: Decadal trends in the North Atlantic Oscillation: Regional temperatures and precipitation. *Science*, **269**, 676–679.
- Kalnay, E., and Coauthors, 1996: The NCEP/NCAR 40-Year Reanalysis Project. *Bull. Amer. Meteor. Soc.*, **77**, 437–471.
- Livezey, R. E., and W. Y. Chen, 1983: Statistical field significance and its determination by Monte Carlo techniques. *Mon. Wea. Rev.*, **111**, 46–59.
- Novak, M. J., L. F. Bosart, D. Keyser, T. A. Wasula, and K. D. LaPenta, 2002: Climatology of warm season 500 hPa cutoff cyclones and a case study diagnosis of 14–17 July 2000. Preprints, *19th Conf. on Weather Analysis and Forecasting*, San Antonio, TX, Amer. Meteor. Soc., P1.11.
- Portis, D. H., J. E. Walsh, M. E. Hamly, and P. J. Lamb, 2001: Seasonality of the North Atlantic Oscillation. *J. Climate*, **14**, 2069–2078.
- Serreze, M. C., A. H. Lynch, and M. P. Clark, 2001: The Arctic frontal zone as seen in the NCEP–NCAR reanalysis. *J. Climate*, **14**, 1550–1567.
- White, J. W. C., L. K. Barlow, D. Fisher, P. Grootes, J. Jouzel, S. J. Johnson, M. Stuiver, and H. Clausen, 1997: The climate signal in the stable isotopes of snow from Summit, Greenland: Results of comparisons with modern climate observations. *J. Geophys. Res.*, **102**, 26 425–26 440.
- Wilks, D. S., 1995: *Statistical Methods in the Atmospheric Sciences*. Academic Press, 464 pp.
- Yarnal, B., and H. F. Diaz, 1986: Relationship between extremes of the Southern Oscillation and the winter climate of the Anglo-American Pacific Coast. *J. Climatol.*, **6**, 197–219.